Arch. Metall. Mater. **65** (2020), 4, 1365-1369

DOI: 10.24425/amm.2020.133701

JONG-YOUN SON[1,2], GWANG-YONG SHIN[2], KI-YONG LEE[2], HI-SEAK YOON[1], DO-SIK SHIM[3*]

DEPOSITION CHARACTERISTICS OF HIGH-THERMAL-CONDUCTIVITY STEEL IN THE DIRECT ENERGY DEPOSITION PROCESS AND ITS HARDNESS PROPERTIES AT HIGH TEMPERATURES

Direct energy deposition (DED) is a three-dimensional (3D) deposition technique that uses metallic powder; it is a multi-bead, multi-layered deposition technique. This study investigates the dependence of the defects of the 3D deposition and the process parameters of the DED technique as well as deposition characteristics and the hardness properties of the deposited material. In this study, high-thermal-conductivity steel (HTCS-150) was deposited onto a JIS SKD61 substrate. In single bead deposition experiments, the height and width of the single bead became bigger with increasing the laser power. The powder feeding rate affected only the height, which increased as the powder feeding rate rose. The scanning speed inversely affected the height, unlike the powder feeding rate. The multi-layered deposition was characterized by pores, a lack of fusion, pores formed by evaporated gas, and pores formed by non-molten metal inside the deposited material. The porosity was quantitatively measured in cross-sections of the depositions, revealing that the lack of fusion tended to increase as the laser power decreased; however, the powder feeding rate and overlap width increased. The pores formed by evaporated gas and non-molten metal tended to increase with rising the laser power and powder feeding rate; however, the overlap width decreased. Finally, measurement of the hardness of the deposited material at 25°C, 300°C, and 600°C revealed that it had a higher hardness than the conventional annealed SKD61.

Keywords: Direct Energy Deposition, HTCS-150, Pore, Lack of Fusion, Hardness

1. Introduction

Three-dimensional (3D) deposition techniques have recently become widely used in various fields [1]. The direct energy deposition (DED) technique is a 3D deposition technique that uses metallic materials; it can not only minimize thermal effects that cause various defects, but can also enable precise control and permit the fabrication of various shapes [2]. The DED is a multi-bead, multi-layered deposition technique. Each single bead overlaps the previously deposited single bead to deposit a single layer, and the single layer is deposited onto a previously deposited single layer to build a 3D structure [3]. During the multi-layered deposition, each single bead or layer is directly related to the whole structure of the deposition, and the beads and layers depend on the process parameters.

In this study, experimental single bead, single layer (multi-beads), and multi-layer depositions were conducted to examine the deposition characteristics with the process parameters of the DED technique, and defects in the depositions were observed to investigate how the parameters affected them. Moreover, the hardness of the deposition was measured to evaluate their mechanical properties.

2. Experimental procedure

2.1. DED system and its main process parameters

This study used laser-assisted metal deposition equipment, using a CO_2 laser (direct metal tooling MX3). Fig. 1(a) shows a schematic of the DED process. A substrate is irradiated by a laser beam, and a pool of melted material forms. A powdered material is simultaneously fed into the melting pool, and the powder melts instantly. Therefore, a single bead is deposited on the substrate via the solidification of the melted powder. The single bead is deposited onto a substrate first, and another single bead is deposited right next to the previously deposited single bead, with the two beads overlapping one another, as shown in Fig. 1(b). In this way, a complete single layer is deposited, and multiple layers are then built upon additively, layer-by-layer.

[1] CHONNAM NATIONAL UNIVERSITY, DEPARTMENT OF MECHANICAL ENGINEERING, GWANGJU, REPUBLIC OF KOREA
[2] KOREA INSTITUTE OF INDUSTRIAL TECHNOLOGY, SMART MANUFACTURING PROCESS GROUP, GWANGJU, REPUBLIC OF KOREA
[3] KOREA MARITIME AND OCEAN UNIVERSITY, DIVISION OF MECHANICAL ENGINEERING, BUSAN, REPUBLIC OF KOREA

* Corresponding author: think@kmou.ac.kr

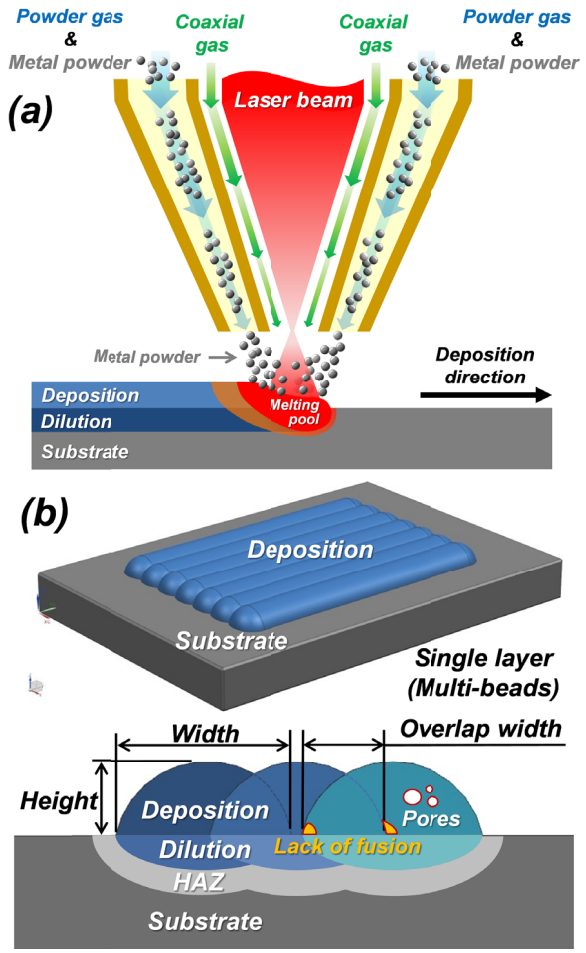

Fig. 1. Schematics of (a) metal deposition in the DED process, and (b) single layer (multi-bead) deposition with defects

In this deposition process, the laser power, the scanning speed of laser beam, the feeding rate of metal powder, and the overlap width between each single bead are the main process parameters that can affect deposition. Table 1 lists process parameters and gives controlled ranges of the main parameters for the experimental depositions in this study.

TABLE 1

Process parameters of the DED and controlled ranges of the main parameters

Process parameters	Value
Power of laser beam	600-1000 W
Powder feeding rate	2-6 g/min
Overlap width between beads	0.3-0.7 mm
Laser scanning speed	600-1000 mm/min
Laser beam diameter (fixed)	1 mm
Powder gas (fixed)	2.5 ℓ/min
Coaxial gas (fixed)	8.0 ℓ/min

2.2. Materials

The HTCS-150, a high-thermal-conductivity steel, was deposited onto a substrate of annealed JIS SKD61, a conventional hot work tool steel. Table 2 presents the chemical compositions of the HTCS-150 and the SKD61. The HTCS-150 was developed by Rovalma Co. to improve productivity in hot working processes with high thermal conductivity. It consists of spherical particles with diameters of 50-150 μm, and the substrate of SKD61 had dimensions of 100 × 50 × 10 mm^3.

2.3. Observations on depositions and hardness test at high temperature

To observe the deposition characteristics of the metallic powder in DED process, the deposited materials were cut perpendicular to the substrate and the deposited region. Cross-sections of the cut samples were then observed using an optical microscope. In addition, depth-sensing micro-indentation tests were performed at 25°C, 300°C, and 600°C using a Nikon QM-2 and an Akashi AAV-502 to investigate the hardness properties of the deposited materials.

3. Results and discussion

3.1. Deposition characteristics depending on process parameters

In the single bead depositions, heights and widths became bigger as the laser power increased, as shown in Figs. 2(a), (b), and (c). In the DED process, the melting pool depended on the laser power. As the laser power increased, the size of melting pool increased, but the molten powder in the melting pool also increased. Thus, both the height and width of the single bead increased. The powder feeding rate proportionally affected only the height of the single bead deposition, not the width. The width depended on the size of melting pool, whereas the height depended on amount of fed powder in the melting pool. Therefore, the height of the single bead increased as the powder feeding rate raised. However, the scanning speed was inversely proportional to the deposited bead height. As the scanning speed increased, the amount of fed powder reduced, because there was not enough time to feed powder into the melting pool. Thus, the molten powder diminished, meaning that the heights of the beads decreased.

In the multi-bead depositions, the deposited results depending on the process parameters are identical with the results of the

TABLE 2

Chemical composition of the HTCS-150 and JIS SKD61 materials [wt.%]

Material	C	Si	Mn	P	S	Mo	Cr	Ni	N	V		Cu	W
HTCS-150	**0.32**	0.8	<0.5	<0.03	0.016	4.185	0.064	0.029	0.03	—		**0.03**	**3.09**
SKD61	**0.32**	0.8	<0.5	<0.03	0.03	1.00	4.5	<0.25	0.03	0.8		—	—

single bead deposition described above. Only the height of each deposition increased as the overlap width broadened.

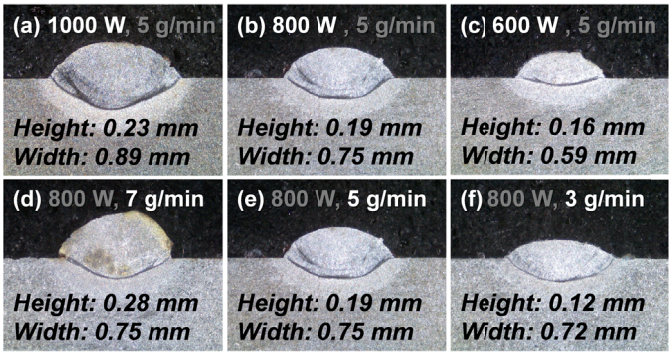

Fig. 2. Heights and widths of single bead depositions under different process parameters: (a), (b), and (c) show controlled laser powers, and (d), (e), and (f) show controlled powder feeding rates

3.2. Pores in the multi-layered depositions

To deposit multi-layered deposition, 5 layers were deposited following a "zigzag" path. Although there were no delaminations or cracks in the multi-layered depositions, several pores were observed in the cross-sections. Fig. 3 shows the pores, divided into a lack of fusion (LOF), pores from evaporated gas, and pores from non-molten metals. To investigate these pores, their areas in the cross-sections of the deposited regions were quantitatively measured using optical microscopes. The pores and lack of fusion were then calculated as shown in Eq. (1):

$$Pores\ and\ LOF\,(\%) = \frac{Area\ of\ pores\ or\ LOF\ (\mathrm{mm}^2)}{Area\ of\ deposited\ region\ (\mathrm{mm}^2)} \times 100 \quad (1)$$

In the laser-assisted metal deposition process, the lack of fusion increases as the laser power decreases, or as the laser scanning speed increases [4]; the amount of heat input in the deposited area is directly linked to the lack of fusion. In the experimental results of the multi-layered depositions, the lack of fusion was observed at the interfaces between the beads, as shown in Fig. 1(b); it is assumed that the adjacent beads in the multi-bead deposition were incompletely fused due to the lack of heat input in the deposited area. The lack of fusion occurred at the interfacial region between the beads. The pores formed by evaporated gas were observed inside the beads; they generally had spherical shapes. These pores were assumed to be formed by evaporated gas. The gas was generated when the metal powder was melted by irradiation of the laser. This gas was not able to escape from the melting pool and was then trapped inside of beads due to the rapidly solidified melted area. Lastly, the pores formed by non-molten metal powder were assumed to be formed by both the lack of heat input in the deposited area and the evaporated gas. The metal powder was excessively fed into the deposited area, and the heat input in the area was not sufficient to melt the excessive powder. The evaporated gas was also simultaneously generated in that of deposited area.

To investigate the relationships between the porosity from the pores and process parameters, contour plots were drawn, as shown in Figs. 4 and 5. Fig. 4 shows contour plots for the lack of fusion and process parameters, and Fig. 5 shows contour plots for the pores formed by evaporated gas and non-molten metal and the process parameters. The lack of fusion tended to increase as the laser power decreased, as the powder feeding rate increased, or as the overlap width broadened. On the other hand, the pores formed by evaporated gas and non-molten metal tended to increase as the laser power increased, as the powder feeding rate increased, or as the overlap width narrowed. These results reveal that the lack of fusion was inversely proportional to the laser power, whereas it was proportional to the powder feeding rate and the overlap width. However, the pores formed by evaporated gas and non-molten metal were proportional to both the laser power and the powder feeding rate, whereas they were inversely proportional to the overlap width.

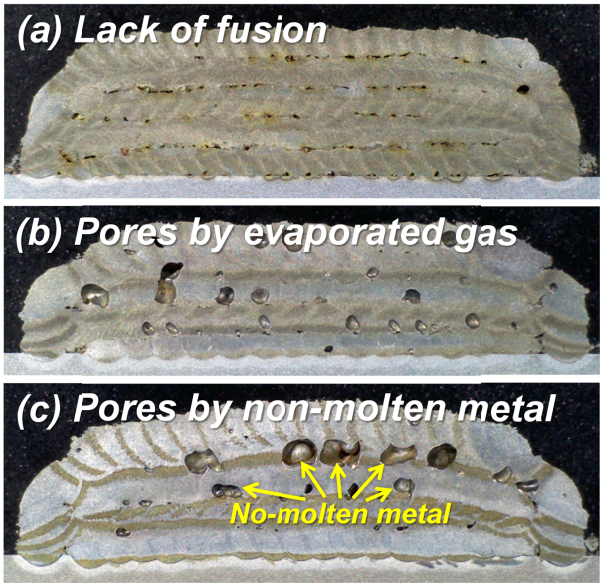

Fig. 3. Pores in the multi-layered depositions, formed by (a) a lack of fusion, (b) evaporated gas, and (c) non-molten metal

3.3. Hardness of deposited HTCS-150

Fig. 6 shows a cross-section of the deposited HTCS-150 and its process parameters for the deposition. This multi-layered deposition had 0.065% of pores with no lack of fusion. To measure hardness distribution, 12 layers of HTCS-150 were deposited onto annealed SKD61 with the process parameters resulting in 0.065% of pores. Fig. 7 shows hardness distribution across the cross-section of deposited HTCS-150 on annealed SKD61 substrate. Hardness was measured over the depth from the top surface of the specimen. These results reveal that the highest hardness occurred in the deposited region and dilution, followed by the HAZ and substrate. The substrate showed an average hardness of 200 HV. The hardness increased rapidly in the HAZ and deposited region. The deposition region showed around 600 HV with no heat-treatment. The hardness of the

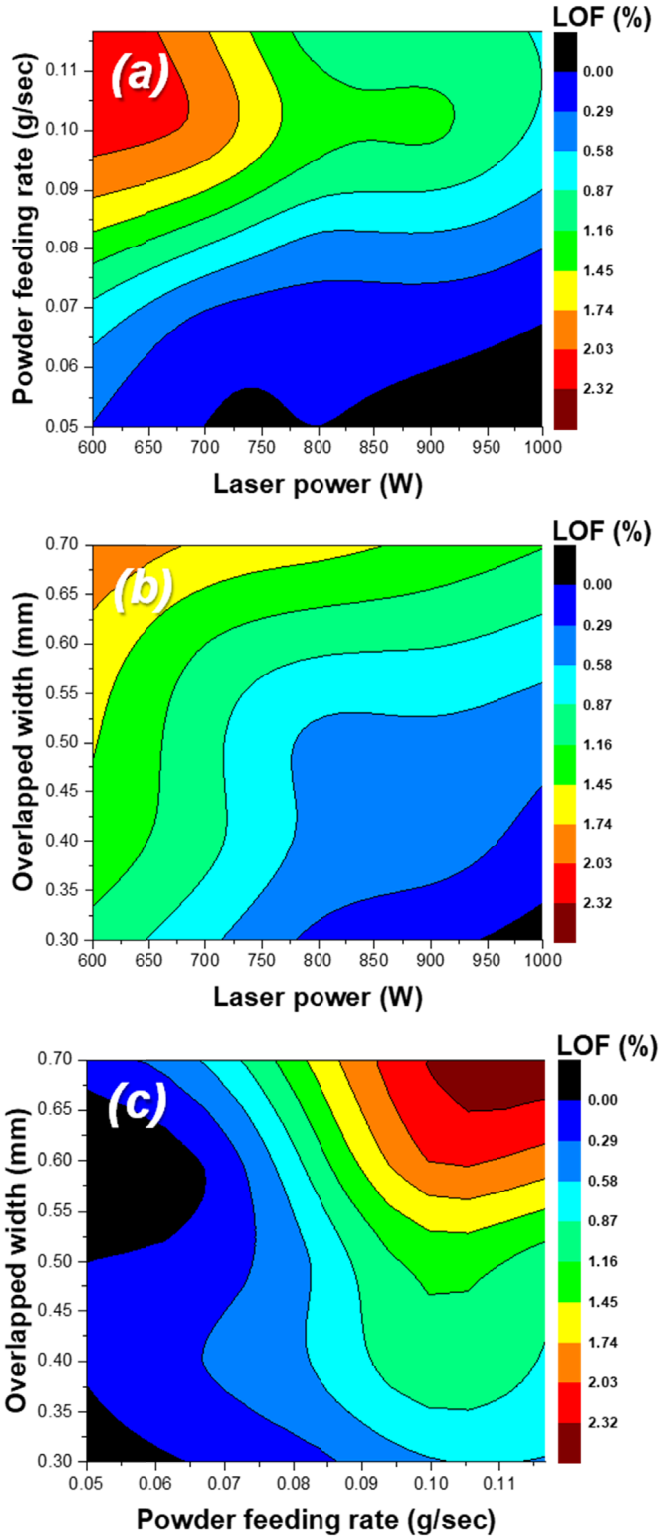

Fig. 4. Contour plots for lack of fusion (LOF) under different process parameters: (a) laser power and powder feeding rate, (b) laser power and overlap width, and (c) powder feeding rate and overlap width

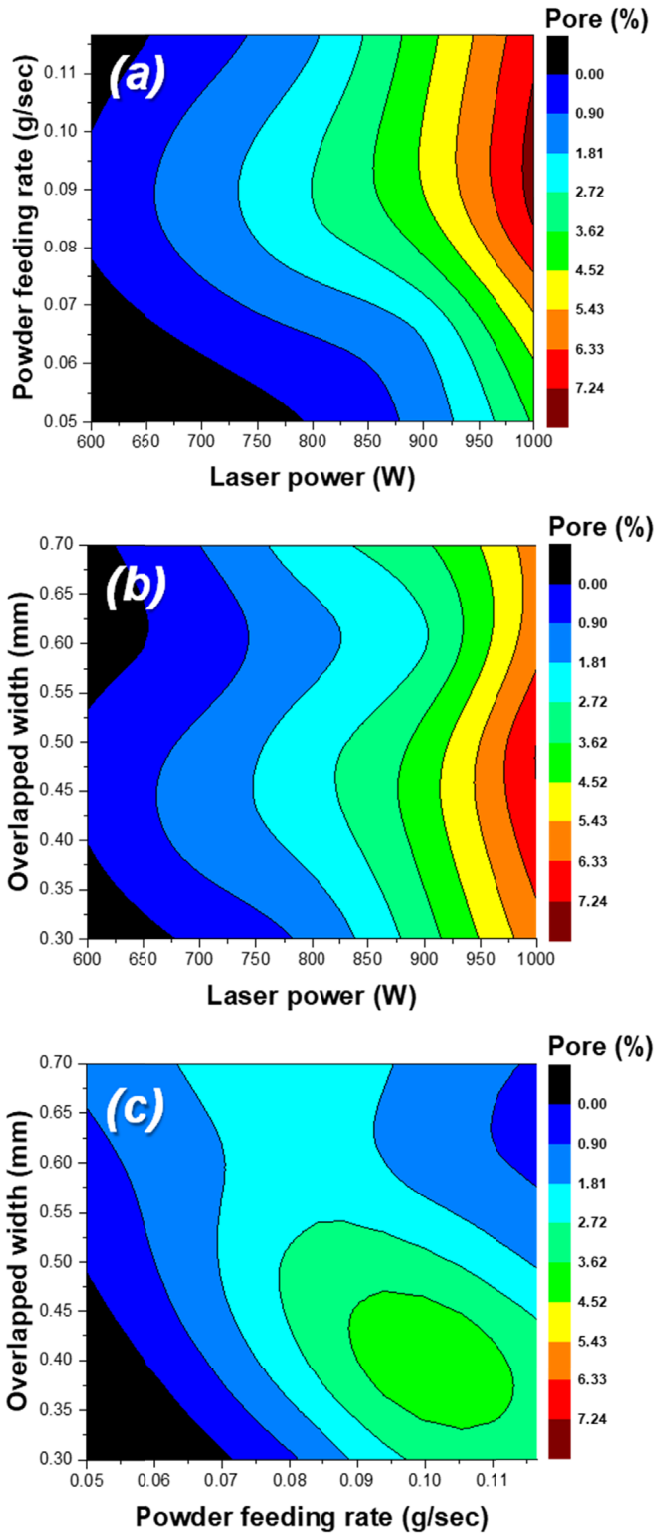

Fig. 5. Contour plots for pores formed by evaporated gas and non-molten metal under different process parameters: (a) laser power and powder feeding rate, (b) laser power and overlap width, and (c) powder feeding rate and overlap width

deposited HTCS-150 was measured at 25°C, 300°C, and 600°C, and its hardness was compared to the annealed SKD61. Fig. 8 shows the hardness graphs of both the deposited HTCS-150 and the SKD61. At 25°C, the SKD61 showed an average hardness of 255 HV, whereas the deposited HTCS-150 showed a higher hardness of 661 HV. The hardness of the deposited HTCS-150 was more than twice that of the SKD61 at 300°C, and was 1.8 times higher at 600°C. These results reveal that the deposited HTCS-150 exhibited higher hardness than the annealed SKD61 at all temperatures.

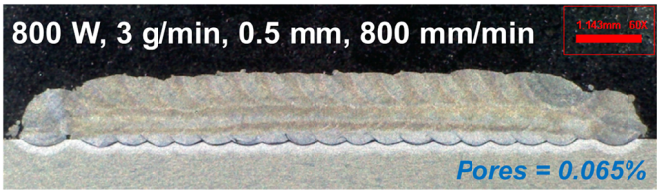

Fig. 6. Multi-layered deposition of the HTCS-150 with the minimum pores and no lack of fusion

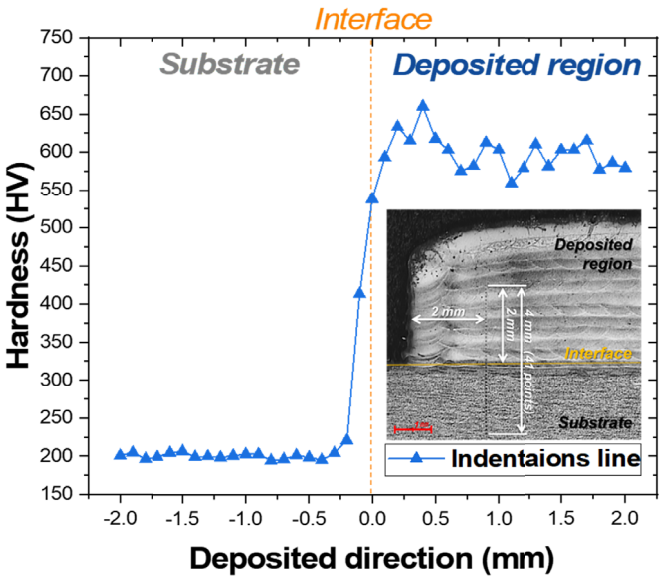

Fig. 7. Hardness distribution on the cross-section of the deposited HTCS-150 on annealed SKD61

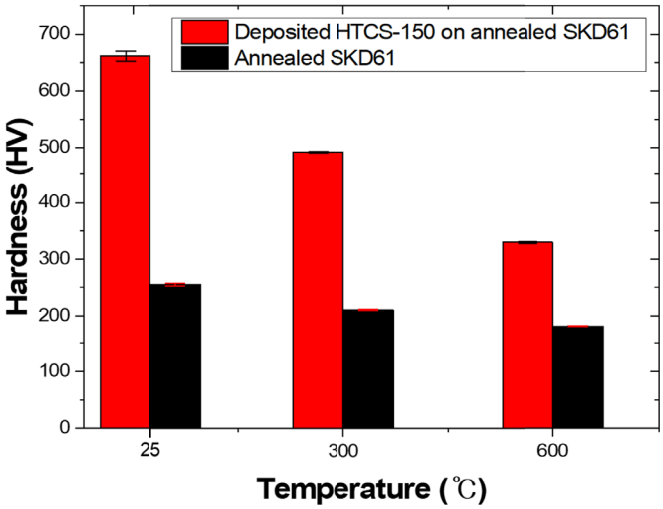

Fig. 8. Hardness at elevated temperatures (25°C, 300°C and 600°C)

4. Conclusions

This study investigated the deposition characteristics of HTCS-150 depending on process parameters in the DED technique. Experimental depositions of single beads revealed that the laser power proportionally affected the height and width of the deposition. The powder feeding rate proportionally affected the height only, but the laser scanning speed was inversely proportional to the height only. In multi-layered deposition experiments, a lack of fusion, pores formed by evaporated gas, and pores formed by non-molten metal were all observed inside the depositions. The lack of fusion was inversely proportional to the laser power but was proportional to the powder feeding rate and overlap width. However, the pores formed by the evaporated gas and non-molten metal were proportional to both the laser power and powder feeding rate, but were inversely proportional to the overlap width. In addition, the deposited HTCS-150 material was compared to annealed SKD61, conventionally use as hot work tool steel, via hardness tests. The deposited HTCS-150 generally exhibited higher hardness than the SKD61 at temperatures of 25°C, 300°C, and 600°C.

Herein, general deposition characteristic and defects in the DED technique were investigated with experimental depositions of HTCS-150. To eliminate the defects on the depositions, dependence of the defects and the process parameters should be numerically analyzed. In the near future, optimization of the parameters will be performed in order to eliminate or reduce the pores in the depositions. In addition, other mechanical properties of deposited material will be examined.

Acknowledgments

This work was supported by the Korea Institute of Energy Technology Evaluation and Planning (KETEP) under grant number 2018201010633B.

REFERENCES

[1] Y.K. Won, Future trend of 3D printing in the center of manufacturing revolution, 3D printing guide **3**, 23 (2017).

[2] M.F. Schneider, Laser cladding with powder, Print Partners Ipskamp (1998).

[3] J.Y. Son, H.Y. Yoon, KY. Lee, S.H. Park, D.S. Shim, Investigation into high-Temperature interfacial strength of heat-Resisting alloy deposited by laser melting process, Met. Mater. Int. 1-11 (2019).

[4] T. Mukherjee, T. DebRoy, Mitigation of lack of fusion defects in powder bed fusion additive manufacturing, Journal of Manufacturing Processes **36**, 442-449 (2018).